www.amlett.com, www.vbripress.com/aml, DOI: 10.5185/amlett.2015.5723 Published online by the VBRI press in 2015

Swift heavy ion irradiation induced surface sputtering and micro structural modification of gold thin films

Priyadarshini Dash[1], Haripriya Rath[1], Udai B. Singh[2], Sunil Ojha[2], Devesh K. Avasthi[2], Naresh C. Mishra[1*]

[1]*Department of Physics, Utkal University, Vani Vihar, Bhubaneswar 751004, India*
[2]*Inter-University Accelerator Centre, Aruna Asaf Ali Marg, New Delhi 110 067, India*

[*]Corresponding author. Tel: (+91) 9437889778; E-mail: nareshcmishra@gmail.com

Received: 26 October 2014, Revised: 21 December 2014 and Accepted: 24 December 2014

ABSTRACT

Two sets of gold thin films of thickness of about 20 and 50 nm, grown by thermal evaporation method on (100) silicon wafers were irradiated by 197 MeV Au ions. Grazing incidence X-Ray diffraction (GIXRD) study has been revealed lattice expansion on decreasing the film thickness. 197 MeV Au ion irradiation was not affect either the cubic crystal structure of gold or its lattice parameter. Atomic force microscopy (AFM) study indicated that the evolution of the surface morphology with ion fluence crucially depended on the film thickness, the thinner film being more sensitive than the thicker one. Irradiation led to nanoparticles formation on the surface of the films. This observation is in contrast to the generally perceived damaging role of swift heavy ion (SHI) irradiation. Power spectral density analysis of the roughness along both the lateral and vertical directions demonstrated dominance of surface diffusion over volume diffusion induced by SHI irradiation. A comparison of the sputtering yield obtained from Rutherford back scattering (RBS) spectra of the irradiated films and transmission electron microscopy (TEM) of the particles sputtered from the films and collected by a catcher grid during irradiation indicated that more than the surface and volume diffusion processes, it is the irradiation induced sputtering that controls the overall surface morphology of the films. The surface roughness increase with ion fluence and the irradiation induced sputtering yield was found to be larger in thinner films. Film thickness dependence of the evolution of surface morphology and sputtering yield with 197 MeV Au ion irradiation clearly indicates the dominance of the electronic energy loss over the nuclear energy loss of the projectiles ions in the target medium and opens up the ways for examining the applicability of different models of ion-matter interaction in systems with reduced dimensions.

Keywords: Ion Irradiation; thermal spike; sputtering; power spectral density; cluster emission.

Priyadarshini Dash is a PhD scholar in the Dept. of Physics, Utkal University, Bhubaneswar, India. Her area of research is synthesis and modification of nanoparticle thin films under swift heavy ion irradiation.

Naresh C. Mishra is a Professor of Physics in Utkal University, Bhubaneswar, India. His research interests include synthesis and study of nanoparticle thin films and bulk materials and evolution of materials under irradiation by high energy heavy ions. He has been member/chairman of many National Research Committees. He has published more than 100 research articles in journals of International/ National repute and has completed many research projects funded by DST, UGC, IUAC and UGC-DAE CSR.

Introduction

An energetic ion traversing through a materials medium looses energy basically through two nearly independent processes: nuclear energy loss dE/dx_n (S_n) due to the elastic collisions of the projectile ions with atoms of the solid and electronic energy loss dE/dx_e (S_e) due to the inelastic collisions with the target electrons [**1**]. In the keV range of the ion energy, the S_n induced processes dominates. In thin films, these processes lead to modification of the surface and interface [**2-6**], which is well understood on the basis of Sigmund's theory [**7**]. When the ion energy is hundreds of MeV, the S_e dominates over S_n in the modification of materials. When the S_e exceeds a materials dependent threshold value, S_{eth}, SHI induce cylindrical amorphized regions called latent tracks along their path in a crystalline matrix. Track formation process occurs in a time scale of a few ps to ns and hence is not directly accessible for

observation by any experimental technique. Several models like thermal spike **[8]**, Coulomb explosion **[9,10]** and more refined models involving statistical deposition of the electronic stopping power **[11]**, role of target inner-shell electron excitation **[12]**, shock waves **[13]**, athermal melting **[14]**, exciton decay **[15]** etc. have been invoked over the years to explain the track formation phenomenon.

In addition to creating amorphized latent tracks, the S_e can lead to modification of the surface morphology of materials **[16-19]** due to two competing phenomena: sputtering and surface diffusion. The first process roughens and the second smoothens the surface. Recent studies have shown that in thin films, the effect of S_e on the surface morphology can be very different from that in thick films and bulk materials **[16]**. A noble metal like gold is known to be insensitive in its bulk state to the S_e induced effects of SHI. It has not been possible to produce latent tracks in gold as in many other highly conducting metals like silver copper, due to the presence of highly mobile conduction electrons. In thin film form however, gold has been shown to have pronounced sensitivity to SHI irradiation. Thinner films of gold for example exhibit larger sputtering as compared to thicker ones under SHI irradiation. Simulations of sputtering yield due to S_n induced effects do not show thickness dependent sputtering. This can arise only due to S_e induced effects of SHI. In this electronic energy loss regime, Sigmund's theory fails to explain the large increase in sputtering yield in thin films **[20].** Though thermal spike model of ion matter interaction has been invoked to explain such observations, exact mechanism is still not clear. A detailed understanding of the electronic sputtering process as well as the diffusion of matter induced by SHI leading to the modifications of the surface morphology is necessary to understand the fundamentals of interaction of ions with the matter.

In the present work, we probe into the structural and morphological modifications and sputtering yield of gold thin films under the impact 197 MeV Au ions. In particular, we have examined the thickness dependent evolution of the surface morphology of gold thin films under both smoothening and roughening effects of SHI irradiation and showed that the evolution of their surface morphology becomes thickness dependent because of the thickness dependence of the sputtering yield under SHI irradiation.

Experimental

Materials and methods of preparation

Gold thin films were deposited on (100) silicon substrates of 1×1 cm^2 size. Deposition was performed in a high vacuum (1.6×10^{-6} mbar) using 99.99% pure gold in the form of wire by thermal evaporation method at the Inter University Accelerator Centre (IUAC), New Delhi. Films were deposited at two different thicknesses (20 and 50 nm). Thickness was measured *in-situ* by quartz crystal monitor and *ex-situ* by Rutherford backscattering spectrometry (RBS).

Ion beam parameters and ion irradiation

The films were bombarded with 197 MeV Au^{8+}ions using the 15 MV Pelletron accelerator at the IUAC, New Delhi. Irradiation was done at three different fluences: (3×10^{12}), (1×10^{13}) and (3×10^{13}) ions cm^{-2}. The ions were incident perpendicular to the surface of the films. The ion beam was scanned over an area of 1×1 cm^2. The vacuum in the chamber during irradiation was 9×10^{-6} mbar.

Characterization techniques

Grazing incidence x-ray diffraction (GIXRD) analysis was performed using Brucker D8 advance x-ray diffractometer with CuK_α radiation (λ= 1.5418 Å) to study crystallinity of the films. GIXRD measurements in the 2θ range of 30° - 80°of the as-deposited as well as irradiated gold films were performed at a grazing angle of 2° with a scan speed of 1° min^{-1}. GIXRD measurements were done at the Department of Physics, Utkal University, Bhubaneswar. Atomic force microscopy (AFM) measurements were done to study evolution of the surface morphology and the microstructure of the films with ion fluence using 'Nanoscope IIIA' atomic force microscope of Digital Instruments at the IUAC, New Delhi. Power spectral density (PSD) analysis was done from the AFM images to extract the mechanisms, which is responsible for the surface morphology under SHI irradiation. Sputtering yield at different fluence was analyzed by *ex-situ* thickness measurement using RBS technique. RBS measurements were performed with 2MeV He^+ ions using 1.7 MV Pelletron facility at the IUAC, New Delhi. The He^+ ions were bombarded on the sample surface and backscattered ions were detected at an angle of 160° to the beam direction using silicon surface barrier detector. The sputtered particles at a fluence of 1×10^{13} ions cm^{-2} were also collected in carbon coated copper TEM grids. The TEM measurements were carried out using 200 kV ultra high resolutions JEOL 2010, UHR facility at the Institute of Physics, Bhubaneswar.

Results and discussion

RBS spectra of the as deposited gold films were analyzed using the Rutherford Universal Manipulation Programme (RUMP) simulation code. The RUMP fitting for RBS spectra (**Fig. 1**) showed that thickness of the two sets of films is around 20 nm and 54 nm as against 20 nm and 50 nm respectively obtained from quartz crystal monitor during deposition.

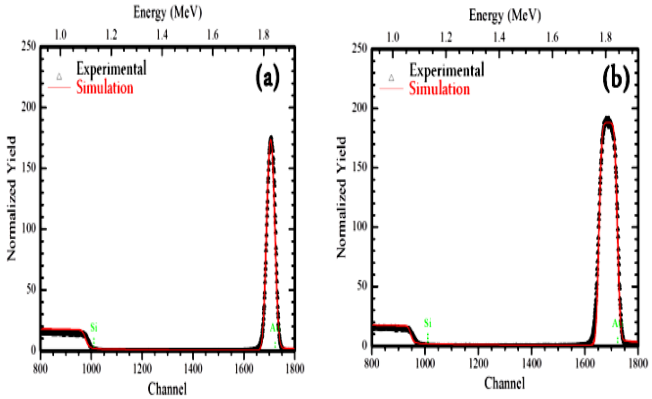

Fig. 1. RBS spectrum of gold on Si along with the RUMP simulated spectrum for (a) 20 and (b) 50 nm films respectively.

The GIXRD pattern (**Fig. 2**) of the as deposited gold thin films and the films irradiated by 197 MeV Au ions at different fluences consist of peaks corresponding to the prominent reflection planes of gold with cubic structure and space group *Fm3m* as reported in the JCPDS files [Card No. 04-0784]. The ratio of the peak intensities match with that reported in JCPDS file indicating polycrystalline nature of the films. Lattice parameter of 4.0684Å for 50 nm and 4.0706Å for 20 nm thin films obtained from the GIXRD spectra indicated lattice expansion on decreasing film thickness as has been reported earlier **[21, 22]**. The crystallite size estimated from the Scherrer equation **[23]** was 15 and 23 nm for 20 and 50 nm thick films respectively. Irradiation did not change these values much.

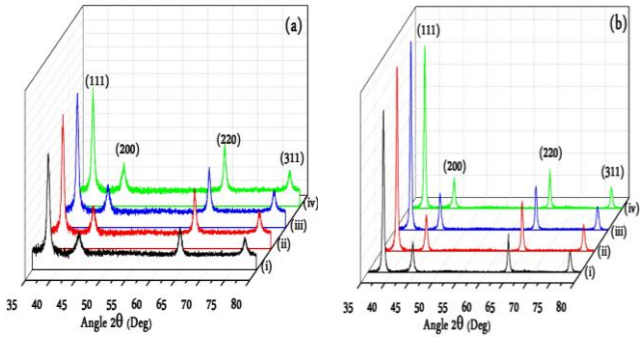

Fig. 2. GIXRD pattern for (i) {(a) 20 and (b) 50 nm} gold films as-deposited as well as irradiated at (ii) 3×10^{12}, (iii) 1×10^{13} and (iv) 3×10^{13} ions cm^{-2} fluences, respectively.

Fig. 3 shows the changes in the surface features induced by 197 MeV Au ion irradiation in gold films of all thicknesses as probed by AFM and their corresponding grain size distribution with irradiation fluence. One µm scan AFM images indicate that the surface of the pristine films exhibits irregular shape grains with wide distribution of grain size for 20 nm thick film, but smooth and featureless for 50 nm thick film. As irradiation proceeds, uniformly distributed nanostructures develop in both the films. The size distribution histograms were obtained from surface profiles of the AFM images for different fluences. With increase of fluence, the average grain size was found to increase up to 1×10^{13} ions cm^{-2} and then decrease for 3×10^{13} ions cm^{-2}. This observations indicate that 197 MeV Au ion irradiation leads to growth of nanoparticles on the surfaces of gold thin films in the low fluence regime and fragmentation of the grains in the high fluence regime.

Fig. 4 presents the surface roughness evolution of 20 and 50 nm gold films as a function of ion fluence obtained from the AFM images. Irradiation did not influence the roughness much in the low fluence regime, but caused a significant increase at the fluence of 3×10^{13} ions cm^{-2}. The increase was more for 20 nm film than for 50 nm film, possibly due to enhanced sputtering for the lower thickness film as discussed later.

AFM images of 1 µm scan size (**Fig. 3**) were utilized for PSD analysis **[24]**. The PSD curves of the as grown and the irradiated surfaces for 20 and 50 nm thick gold films are shown in **Fig. 5**. By fitting the high q region of **Fig. 5** to equation-1**[25]**, we obtain the roughness exponent δ.

$$C(q) = Aq^{-\delta} \quad (1)$$

where, $C(q)$ is the PSD function, A is a constant and δ is the power-law exponent. The evolution of δ with irradiation fluence as obtained using Equation 1 is shown in **Fig. 6**.

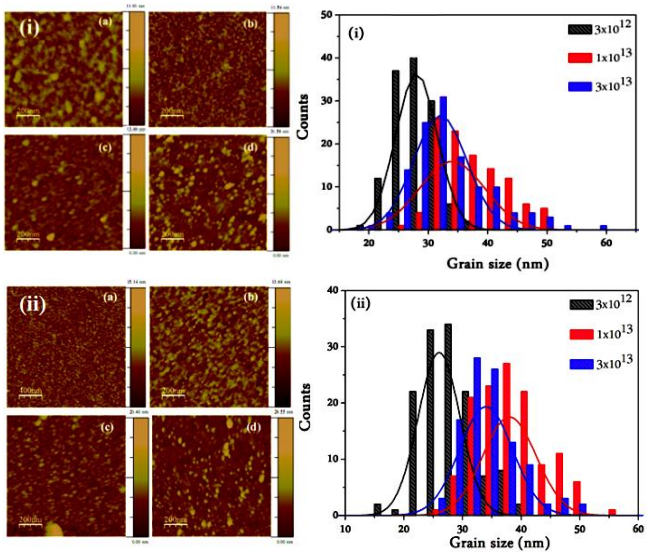

Fig. 3. 1µm× 1µm AFM images of Pristine (i. a) 20 and (ii. a) 50 nm gold films and irradiated by 197MeV Au ion at {**(b)** 3×10^{12} **(c)** 1×10^{13} **(d)** 3×10^{13}} ions cm^{-2}, and their corresponding grain size distribution at different fluences.

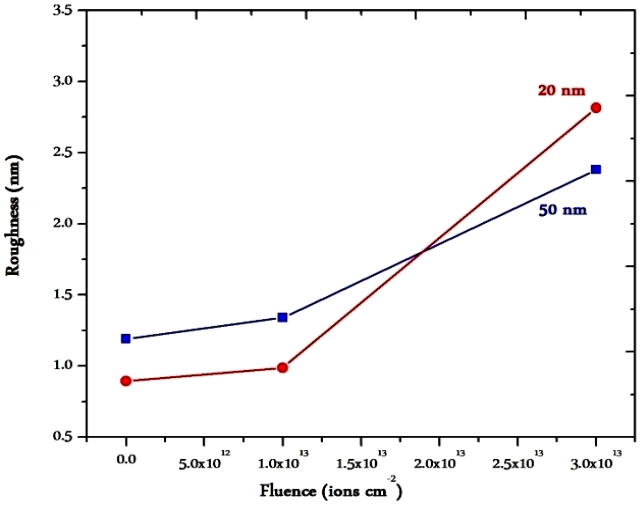

Fig. 4. Roughness variation of 20 and 50 nm gold films with 197 MeV Au ion irradiation.

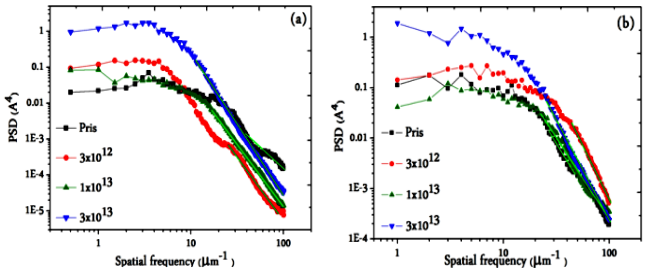

Fig. 5. Plots of PSD versus spatial frequency q of (a) 20 and (b) 50 nm pristine gold surface as well as that irradiated at different fluences by 197MeV Au ion.

The value of δ indicates the mechanisms, which is responsible for the irradiation induced changes in the surface morphology **[26]**. In the present study the value of δ

for all irradiation fluences lies between 3 and 4, which indicate that the surface morphologies are governed by the combined effect of volume diffusion and surface diffusion processes. The increase of δ value towards 4 under 197 MeV Au ion irradiation indicates that the surface diffusion becomes dominant over volume diffusion in the high fluence regime.

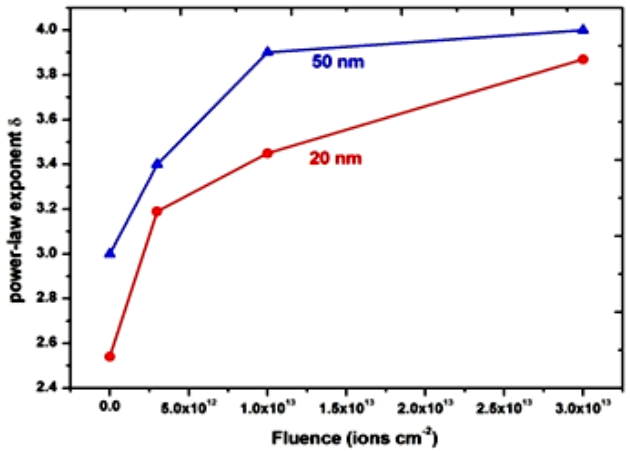

Fig. 6. Variation of power-law exponent δ with ion fluence for both 20 and 50 nm gold films.

The magnified view of the RBS spectra due to gold (20 and 50 nm) (**Fig. 7**) clearly reveals reduction of thickness of the films with 197 MeV Au ion irradiation fluence. This can occur due to erosion of atomic and molecular species from the surface under ion impingement **[27, 28]**. To probe further into the sputtering dependence on thickness of the films under 197 MeV Au irradiation, the sputtering yield or Y (atoms/ion) of gold atoms was determined by using equation- 2 **[29]**.

$$Y\left(\frac{atoms}{ion}\right) = \frac{\Delta N\left(\frac{atoms}{cm^2}\right)}{\Delta f\left(\frac{ions}{cm^2}\right)} \qquad (2)$$

where ΔN is the change in areal concentration (atoms/cm^2) at two different fluences and Δf is the difference in corresponding fluence (ions/cm^2) values. The gold atoms retained in the films after each fluence of 197 MeV Au ion irradiation was estimated from the change in areal concentration with ion fluence (**Fig. 7**). The sputtering yield thus estimated, was 531 and 350 atoms per Au ion for 20 and 50 nm thick films respectively. The electronic (S_e) and nuclear (S_n) energy losses of 197 MeV Au ions in gold as obtained from SRIM (stopping and range of ions in matter) simulation, are 51 keV nm^{-1} and 0.69 keV nm^{-1} respectively. The sputtering yield due to S_n for 197 MeV Au ion in gold also obtained from SRIM, is 2 atoms per incident ion. The much larger sputtering yield than what is predicted by the S_n induced process seen in our case thus arises due to electronic energy loss (S_e). Further, thickness of the films has been found to be crucial parameter in determining the sputtering yield. The thinner films showed higher sputtering yield as compared to the thicker films. Gupta and Avasthi found the sputtering yield of 410 atoms per ion for 15 nm thick gold films and 235 atoms per ion in 45 nm thick gold film at 1×10^{13} ions cm^{-2} fluence for 200 MeV Ag ion irradiation **[16]**. This result along with ours clearly establishes S_e induced sputtering phenomenon in gold thin films.

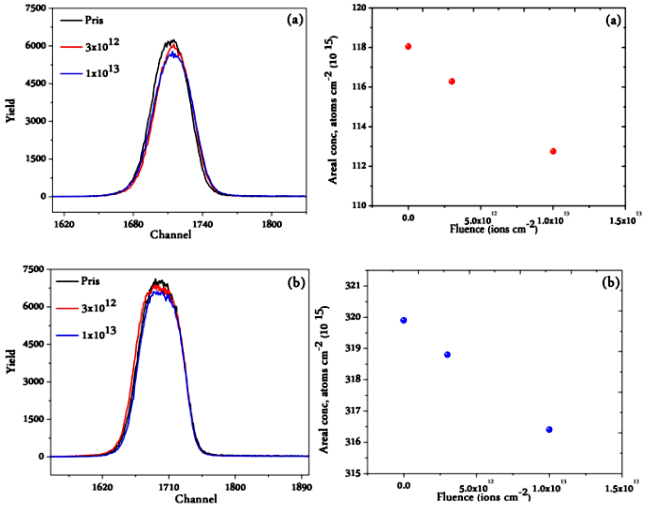

Fig.7. Evolution of RBS spectra and variation of areal concentration with irradiation fluence for (a) 20 and (b) 50 nm gold films.

Sputtered gold nano particles from gold thin films irradiated by 197 MeV Au ions were collected in carbon coated copper catcher grids. Transmission electron microscopy (TEM) images of gold nano particles collected by catcher grids at the fluence of 1×10^{13} ions cm^{-2} for 20 and 50 nm thick films are shown in **Fig. 8**. The size distributions of the particles on the catcher grids of 20 nm and 50 nm films are also shown in **Fig. 8**. The average size of the sputtered particles was found to decrease from 11 nm for 20 nm thick film to 7 nm for 50 nm thick film on irradiation at the fluence of 1×10^{13} ions cm^{-2}.

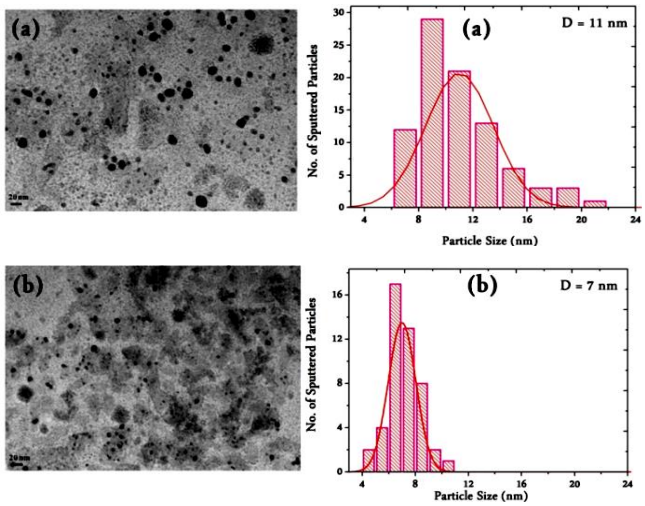

Fig. 8. TEM images and size distribution of sputtered nanoparticles collected on catcher grid at a fluence of 1×10^{13} ions cm^{-2} from (a) 20 nm and (b) 50 nm gold films respectively.

The larger size of gold nanoparticles in thinner film again re-emphasized the importance of thickness dependence of S_e induced sputtering yield in thin films. The high resolution transmission electron microscopy (HRTEM) images of a sputtered nanoparticle (**Fig. 9 (a)**) and its electron diffraction pattern (**Fig. 9 (b)**) reveal the

crystalline nature of the nanoparticles, and the spacing between two consecutive lattice planes (0.219 nm) corresponds to that of the (111) planes of gold.

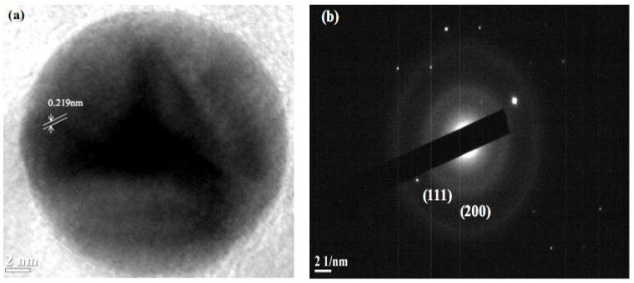

Fig. 9. (a) HRTEM Micrograph of gold nano particle and (b) Selected area diffraction pattern of nano particles collected in catcher grid.

The unsolved mechanisms behind electronic sputtering during ion irradiation have attracted considerable experimental and theoretical attention. In particular, much interest has been devoted to understand the basic mechanisms behind creation of large clusters containing 100 or more atoms and ejection of such large entities during ion irradiation. In the MeV range, ejection of species has been observed with SHI irradiation on thin films **[30, 31]**. This has been explained on the basis of confinement of energy spikes within the grains and thin films induced by ions. In present case, collected gold nanoparticles on catcher grids for 20 and 50 nm thick films at the fluence of 1×10^{13} ions cm^{-2} with irradiation of 197 MeV Au ions can be understood on the basis of thermal spike induced shock waves or pressure pulses due to ion impact **[32]**. Beyond a critical value of pressure generated due to shock waves, cluster of gold ions seem to get ejected out from the surface of the gold thin film, which are collected as nanoparticles on the catcher grid. Confinement of the energy deposited by SHI in thin films explains the observed larger size of nanoparticles emitted from thinner film.

Conclusion

This study has shown that while swift heavy ion irradiation does not influence the crystal structure and the crystallite size of gold thin films much, it greatly influences the surface morphology. The surface evolves under the combined influence of surface diffusion and sputtering leading to smoothening and roughening respectively. The later process was found to dominate at higher ion fluences, with a consequent large increase of roughness. Lowering of film thickness led to enhanced sputtering and larger increase of roughness with ion fluence, thus indicating the importance of the confinement of SHI induced thermal spike in the reduced dimension of the films. SHI irradiation also led to formation of nano-particles on the surface of the films as well as on the catcher grids used to collect the sputtered particles. Since SHI induced sputtering process in a thin films, in addition to being dependent on film thickness, can also depend on other target and projectile related parameters like surbstrate characteristics, mass and charge state of the projectile ions etc. Further studies in this direction may shed light on the details of ion-matter interaction mechanism.

Acknowledgements

One of the authors P. Dash would like to thank the Council of Scientific and Industrial Research (CSIR), New Delhi, Government of India for financial support through senior research fellowship. The authors are thankful to the IUAC, New Delhi Pelletron group for providing a good quality scanned beam for irradiation.

Reference

1. Lindhard, J. and Schad, M.; *Phys. Rev.*, **1961,** *124*, 128. **DOI:** 10.1103/PhysRev.124.128
2. Mantl, S.; Rehn, L. E.; Averback, R. S.; Thompson, L. J. Jr.; *Nucl. Instrum. MethodsPhys. Res. B*, **1985**, *8*, 622. **DOI:** 10.1016/0168-583X(85)90444-6
3. Shreter, U.; Frank, C. T. So, Nicolet. M. A. *J. Appl. Phys.*, **1984**, *55*, 3500. **DOI:** 10.1063/1.332938
4. Ogale, S. B.; Joshee, R.; Godbole, V. P.; Kanetkar, S. M.; Bhide, V.G.; *J. Appl. Phys.*, **1985**, *57*, 2915. **DOI:** 10.1063/1.335231
5. Averback, R. S.; Thompson, L. J. Jr.; Moyle, J.; Schalit, M.; *J. Appl. Phys.*, **1982**, *53*, 1342. **DOI:** 10.1063/1.330624
6. Lee, R.Y.; Whang, C. N.; Kim, H. K.; Smith, R. J.; *Nucl. Instrum. Methods Phys. Res. B*, **1988**, *33*, 661. **DOI:** 10.1016/0168-583X(88)90654-4
7. Sigmund, P.; *Phys. Rev.*, **1969**, *184*, 383. **DOI:** 10.1103/PhysRev.184.383
8. Bonfiglioli, G.; Ferro, A.; Mojoni, A.; *J. Appl. Phys.*, **1961**, *32***,** 2499. **DOI:** 10.1063/1.1728339
9. Fleischer, R. L.; Price, P. B. and Walker, R. M.; *J. Appl. Phys.*, **1965**, *36***,** 3645. **DOI:** 10.1063/1.1703059
10. Lesueur, D and Dunlop, A.; *Radiat. Eff. Defects Solids*, **1993,** *126*, 163. **DOI:** 10.1080/10420159308219701
11. Dartyge, E and Sigmund, P.; *Phys. Rev. B*, **1985**, *32***,** 5429. **DOI:** 10.1103/PhysRevB.32.5429
12. Tombrello, T. A.; *Nucl. Instr. and Meth. B*, **1984**, *2***,** 555. **DOI:** 10.1016/0168-583X(84)90265-9
13. Kitazoe, Y.; Hiraoka, N and Yamamura, Y.; *Surf. Sci.*, **1981**, *111*, 381. **DOI:** 10.1016/0039-6028(81)90396-4
14. Stampfli, P and Bennemann, K. H.; *Phys. Rev. B***, 1990**, *42*, 7163. **DOI:** 10.1103/PhysRevB.42.7163
15. Agullo-Lopez, F.; Mendez, A.; Garcia, G.; Olivares, J and Cabrera, J. M.; *Phys. Rev. B***, 2006**, *74*, 174109. **DOI:** 10.1103/PhysRevB.74.174109
16. Gupta, A.; Avasthi, D.K.; *Physical Review B*, **2001**, *64*, 155407. **DOI:** 10.1103/PhysRevB.64.155407
17. Skuratov, V. A.; Zinkle, S. J.; Efimov, A. E.; Havancsak, K.; *Nucl. Instrum.Methods Phys. Res. B*, **2003**, *203*, 136. **DOI:** 10.1016/S0168-583X(02)02197-3
18. Thomas, S.; Thomas, H.; Avasthi, D. K.; Tripathi, A.; Ramanujan, R.V. and Anantharaman, M. R.; *Journal of Applied Physics*, **2009,** *105*, 033910. **DOI:** org/10.1063/1.3075581
19. Srivastava, S. K.; Avasthi, D. K.; Assmann, W.; Wang, Z. G.; Kucal, H.; Jacquet, E.; Carstanjen, H. D. and Toulemonde, M.; *Physical Review B*, **2005**, *71*, 193405. **DOI:** 10.1103/PhysRevB.71.193405
20. Chaumont, J.; Bernas, H.; Kusnetsov, A.; Clerc, C.; Damoulin, L.; *Nucl. Instrum. Methods Phys. Res. Sect. B*, **1997**, *129*, 436. **DOI:** 10.1016/S0168-583X(97)00350-9
21. Siegel, J.; Lyutakov, O.; Rybka, V.; Kolska, Z.; Svorcik, V.; *Nanoscale Research Letters*, **2011**, *6*, 96. **DOI:** 10.1186/1556-276X-6-96
22. Kolska, Z.; Riha, J.; Hnatowicz, V.; Svorcik, V.; *Materials Letters*, **2010**, *64*, 1160. **DOI:** 10.1016/j.matlet.2010.02.038
23. Culity, B. D.; Element of X-ray Diffraction; MA Reading: Addison-Wesley, **1978.**

24. Dash, P.; Mallick, P.; Rath. H.; Tripathi, A.; Prakash, J.; Avasthi, D. K.; Mazumdar, S.; Varma, S.; Satyam, P. V. and Mishra, N. C.; *Appl. Surf. Sci*, **2009**, *256*, 558.
DOI: 10.1016/j.apsusc.2009.08.046
25. Eklund, E. A.; Snyder, E. J.; Williams, R. S.; *Surf. Sci*, **1993**, *285*, 157.
DOI: 10.1016/0039-6028(93)90427-L
26. Herring, C.; *J. Appl. Phys*, **1950**, *21*, 301.
DOI: org/10.1063/1.1699658
27. Kumar, M.; Rajput, P.; Khan, S. A.; Avasthi, D. K.; Pandey, A. C. *Appl. Surf. Sci.* **2010,** *256*, 2199.
DOI: 10.1016/j.apsusc.2009.09.073
28. Pannu, C.; Singh, U. B.; Agarwal, D. C.; Khan, S. A.; Ojha, S.; Chandra, R.; Amekura, H.; Kabiraj, D.; Avasthi, D. K.; *Beilstein J. Nanotechnol.*, 2014, *5*, 1691.
DOI: 10.3762/bjnano.5.179
29. Rossnagel, S.; Handbook of Thin Film Deposition Processes and Techniques; William Andrew; **2001**, pp.319.
30. Singh, U. B.; Agarwal, D. C.; Khan, S. A.; Mohapatra, S.; Tripathi, A. and Avasthi, D. K.; *J. Phys. D: Appl. Phy*, **2012**, *45*, 445304.
DOI: 10.1088/0022-3727/45/44/445304
31. Pandey, R. K.; Kumar, M.; Singh, U. B.; Khan, S. A.; Avasthi, D. K. and Pandey, A. C.; *Nucl. Instrum. Methods Phys. Res. B*, **2013**, *314*, 21.
DOI: 10.1016/j.nimb.2013.03.060
32. Bitensky, I. S.; and Parilis, E. S.; *Nucl. Instrum. Methods Phys. Res. B*, **1987**, *21*, 26.
DOI: 10.1016/0168-583X(87)90135-2